Fractal Model of Radon Emanation from Solids

Thomas M. Semkow

Wadsworth Center for Laboratories and Research, New York State Department of Health, Albany, New York 12201-0509 and State University of New York at Albany, Albany, New York 12222

(Received 18 March 1991)

A fractal model of radon emanation from solids was developed, based on α recoil from the α decay of radium. Range straggling of the recoiling radon atoms in the solid state was included and the fractal geometry was employed to describe the roughness of the emanating surface. This allowed derivation for the first time of the relation between the radon emanating power and the specific surface area as measured by the gas adsorption. It is suggested that emanating-power measurements can be used to determine the fractal dimensions of surfaces on the scale from tens to hundreds of nanometers.

PACS numbers: 61.16.−d, 23.90.+w, 34.50.Bw, 89.60.+x

There has been a renewed interest in Rn research during the last decade or so triggered by the realization that the Rn daughters are a primary source of the natural-radiation dose delivered to the general population.[1] Most of that research has been focused on geological and health-related aspects. In this paper we describe the physical basis for Rn emanation, which makes the Rn atoms available for other processes. It is well established that at room temperature Rn emanates from solids by α recoil from the α decay of Ra.[2] Owing to recoil energies ~ 100 keV, the ranges of Rn atoms in solids are merely of the order of tens of nm. Consequently, the ejection of Rn atoms into the air space can occur from a solid region close to the surface, which makes the emanation an essentially surface phenomenon. Attempts to relate the emanating power E_R to the surface-to-volume ratio S/V or the specific surface area A of the emanating solid have been made using Euclidean geometry[2,3] (emanating power is referred to as a fraction of Rn atoms that emanated under steady-state conditions). They resulted in the relation

$$E_R = \tfrac{1}{4} RS/V = \tfrac{1}{4} R\rho_0 A, \quad r_0 \gg R, \tag{1}$$

where R is an extrapolated range of Rn in the solid, r_0 is the radius (the half size) of the emanating grain (solid), ρ_0 is the solid-state density, and an assumption of uniform distribution of Ra in the solid was made. In a preliminary work we found discrepancies between Eq. (1) and experiments as high as a factor of 31 for specific surface area of several hundreds $m^2 g^{-1}$, and we attributed them to the use of extrapolated rather than median projected ranges, the Euclidean character of Eq. (1), as well as Rn implantation effects.[4] In this paper we discuss the range straggling of recoiling Rn atoms in emanation from a plate, followed by a development of a fractal model of Rn emanation based on the fractal geometry of Mandelbrot.[5] This yields the proper relations between E_R and S/V as well as r_0 for the first time. In addition, we discuss the processes associated with emanation, such as Rn-atom implantation and indirect recoil, as well as suggest a new process of penetrating recoil.

We consider an isotropic α decay of ^{224,226}Ra in the solid. The recoil energies E_0 are 103 and 86 keV for ^{220}Rn and ^{222}Rn, respectively. Rn atoms lose their energies in the elastic collisions with atoms of the solid (nuclear stopping). Because of the range straggling, the recoiling atoms will stop at a distance between 0 and $2R_m$ from the point of decay, where R_m is a median projected range in the solid. Assuming a Gaussian range straggling and neglecting the angle straggling as well as channeling effects, the normalized probability of finding the Rn atom in the solid at a distance r from the decay point is given by

$$W(r) = \frac{1}{4\pi r^2} \frac{1}{\sqrt{2\pi}\sigma_m} e^{-(r-R_m)^2/2\sigma_m^2} \Big/ \operatorname{erf}\left[\frac{R_m}{\sqrt{2}\sigma_m}\right], \tag{2}$$

where the error function $\operatorname{erf}(t)$ is introduced.[6] The R_m and σ_m can be calculated from the Lindhard, Scharff, and Schiøtt (LSS) theory of energy loss by keV ions.[7] Some of the recoils will lead to emanation at the air-solid boundary as illustrated in Fig. 1 by an arrow. We consider the emanation from an infinite plate of half thickness r_0. The Rn emanating power is calculated by integrating Eq. (2) over the spherical segment protruding from the solid (see Fig. 1) and averaging over the volume of the plate. For $r_0 < 2R_m$ we have to include

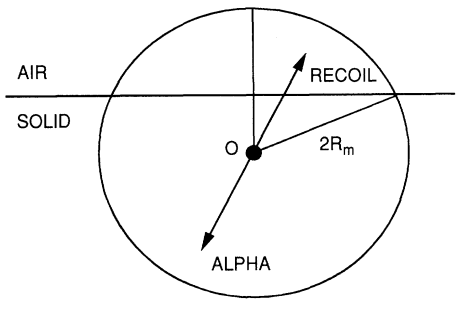

FIG. 1. Rn emanation from plate for α decay of Ra at point O. R_m is the median projected range of the recoil in the solid.

the emanation from both sides of the plate. The result is

$$E_R = 1/4x, \quad x \geq 1, \tag{3a}$$

$$E_R = \frac{1}{2}(1-x) + \frac{1}{8x} - \frac{(1-2x)^2 \operatorname{erf}[b(1-2x)]}{8x \operatorname{erf}(b)} - \frac{e^{-b^2(1-2x)^2} - e^{-b^2}}{8\sqrt{\pi} b x \operatorname{erf}(b)} + \frac{x}{2\sqrt{\pi} b \operatorname{erf}(b)} \sum_{n=0}^{\infty} b^{-n} \left[\gamma\left(\frac{n}{2}+1, b^2\right) - \gamma\left(\frac{n}{2}+1, b^2(1-2x)^2\right) \right], \quad x < 1, \tag{3b}$$

where the reduced variables $x = r_0/R_m$ and $b = R_m/\sqrt{2}\sigma_m$ are used and the incomplete γ function $\gamma(s,t)$ is applied.[6] The leading terms in Eqs. (3) are

$$E_R = 1/4x, \quad x \geq 0.5, \tag{4a}$$

$$E_R = 1 - x, \quad x < 0.5. \tag{4b}$$

The differences between Eqs. (3) and (4) are $\leq 8\%$, which justifies further use of Eqs. (4), especially considering the other assumptions made.

To describe the emanation from a realistic rough surface we assume that it is self-similar. It is a reasonable assumption considering that a majority of surfaces have been found to be self-similar in the molecular range. As before, we consider an infinite plate of half thickness r_0 with a fractal surface such as the one depicted in Fig. 2. The direct recoil is denoted by the arrow labeled 1. Other processes from Fig. 2 will be discussed later. It is seen from Fig. 2 that a considerable porosity is associated with the fractal surface. It has been shown by Pfeifer *et al.* that the pore-size distribution scales as Br^{-D-1}, where r is the radius of the pore, D is the fractal dimension of the surface, and B is a constant.[8] Considering the fact that the pore space above the fractal surface is a "negative" of the solid-state space, we can say that the solid state is built from the features that bear the same distribution as the pores. We calculate the volume-integrated Rn escape probability E as the integral over the above feature-size distribution using plates as the geometrical model for emanation [Eqs. (4)] and feature volumes given by Kr^3 for $2r < R_m < 2r_0$, Kr^3 for $R_m < 2r < 2r_0$, and $Kr^2 r_0$ for $R_m < 2r_0 < 2r$, where K is a constant. We get

$$E = \int_0^{R_m/2} \left(1 - \frac{r}{R_m}\right) Kr^3 B r^{-D-1} dr + \int_{R_m/2}^{r_0} \frac{R_m}{4r} Kr^3 B r^{-D-1} dr + \int_{r_0}^{\infty} \frac{R_m}{4r_0} Kr^2 r_0 B r^{-D-1} dr = \frac{KB}{(3-D)(D-2)} \frac{2^{D-3}}{4-D} R_m^{3-D}. \tag{5}$$

In deriving Eq. (5) we made two assumptions. We neglected the edge effects in emanation from plates.[2] We also assumed that, when the solid-state features are stacked together, there is a mutual cancellation of terms corresponding to recoils that do not fall outside the surface boundary. The coefficient in front of Eq. (5) can be deduced using a technique of Pfeifer *et al.*[8] The surface is covered with a monolayer of adsorbate molecules and the monolayer volume $V(a)$ is given by

$$V(a) = \frac{KB}{(3-D)(D-2)} a^{3-D}, \tag{6}$$

where a is the diameter of an adsorbate molecule, e.g., $a \approx 3.5$ Å for the N_2 molecule. Combining Eqs. (5) and (6) we get

$$E = \frac{2^{D-3}}{4-D} V(a) \left(\frac{R_m}{a}\right)^{3-D} = \frac{2^{D-3}}{4-D} V(R_m). \tag{7}$$

In Eq. (7), $V(R_m)$ is the three-dimensional content[5] (actually one-half of it) of the fractal surface for the covering ball radius R_m. It is obtained by centering a circle at each point of the fractal and taking the outer hull of the circles shown in Fig. 2 as a solid curve at a distance R_m from the fractal surface.

The emanating power is the ratio of E to the solid-state volume V, since a uniform distribution of Ra was assumed. Using Eq. (7) as well as $V(a) = aS$, where S is the Brunauer, Emmett, and Teller (BET) value of the

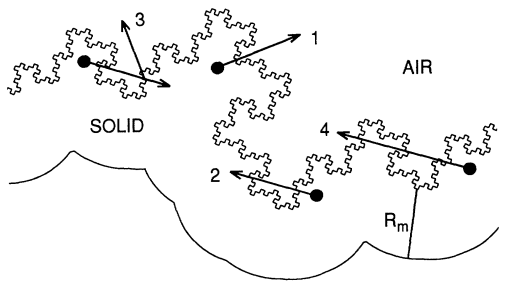

FIG. 2. Rn emanation from the fractal surface. Arrows denote the following processes: 1, direct recoil; 2, implantation; 3, indirect recoil; and 4, penetrating recoil.

surface area, one obtains

$$E_R = \frac{1}{4}\left[\frac{2^{D-1}}{4-D}\left(\frac{a}{R_m}\right)^{D-2}\right] R_m \frac{S}{V}, \quad 2r_0 \geq R_m . \tag{8a}$$

Using a similar procedure one obtains

$$E_R = 1 - \frac{3-D}{4-D}\frac{2r_0}{R_m}, \quad R_m > 2r_0 . \tag{8b}$$

Equation (8a) can be expressed as a function of the half thickness of the solid r_0. Substituting $S/V = Cr_0^{D-3}a^{2-D}$, we obtain

$$E_R = \frac{C}{4-D}\left(\frac{R_m}{2r_0}\right)^{3-D}, \quad 2r_0 \geq R_m , \tag{9}$$

where C is a shape coefficient ($C=1$ for a plate). As expected, substituting $D=2$ we obtain the following Euclidean formulas: Eq. (1) from Eq. (8a), Eq. (4a) from Eq. (9), and Eq. (4b) from Eq. (8b), respectively. For $D=3$ Eqs. (8) and (9) all yield complete emanation ($E_R=1$). For $D=3$ the surface is formally composed of a unimolecular layer of solid that completely fills the space. Therefore all Rn would formally emanate from it (but also be trapped). Real surfaces with D close to 3 do not fill the space, however. The surface is composed of thin solid sections with well-developed microporosity, enabling Rn to emanate.

Equation (9) shows that the emanating power should scale as r_0^{D-3}. Therefore from a logarithmic plot of E_R versus the size, one should be able to deduce the fractal dimension of the emanating surface. We illustrate this point by plotting in Fig. 3 the emanation results from materials of geological origin. Barretto[9] measured the emanating powers of ^{222}Rn from sieve-separated size fractions of Lipari volcanic glass (squares). The E_R values in the vicinity of 10^{-2}–10^{-3} are characteristic of a uniform distribution of ^{226}Ra, for grain sizes of the order of several μm. The straight line is a least-squares fit to the data. From the slope of -0.83 ± 0.06 we get a value of $D = 2.17 \pm 0.06$. It is noteworthy that, while the gas-adsorption technique is sensitive to the region of self-similarity between fractions of nm to tens of nm, the emanation technique is sensitive to self-similarity in the range $(R_m/2, R_m r_{max}/2r_{min})$, where r_{min} and r_{max} are the minimum and maximum radii of particles studied, for a particle with radius r_{max}. Applying these concepts to the data of Barretto[9] and using $R_m = 26$ nm, $r_{min} = 47$ μm, and $r_{max} = 1000$ μm, we get a range of self-similarity between $\sim$13 and $\sim$280 nm. The emanation technique for D determination thus complements the adsorption technique by being sensitive between tens and hundreds of nm. The other data plotted in Fig. 3 are for ^{222}Rn (triangles) and ^{220}Rn (diamonds) emanation from pitchblende.[10] The least-squares fits yield a value of $D = 2.83 \pm 0.03$.

To illustrate a dependence of E_R on A we plot in Fig. 4 the data of Quet and Bussière[11] for the ^{220}Rn emanation from MgO containing ^{224}Ra. The specific surface areas were measured by N_2 adsorption. The curve in Fig. 4 has a linear section, between points 8 and 16, and it deviates from linearity between points 1 and 7. The slope E_R/A of the linear section is about 25 times lower than the one predicted by the Euclidean formula [Eq. (1)]. Points 7 and 1 can also be assigned "slopes" which results in the discrepancy factors of 26 and 31, respectively. A can increase when r_0 decreases or D increases. We thus conclude from Eq. (8a) that the linear section in Fig. 4 has a constant D and a decreasing r_0, while the deviation from linearity corresponds to both an increase in D and a decrease in r_0. This is supported by our es-

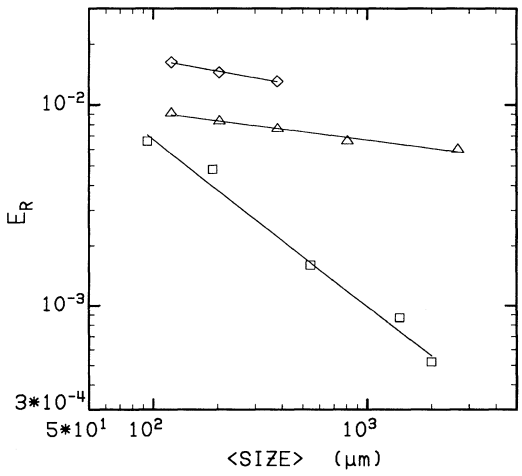

FIG. 3. Emanating power E_R plotted vs the average size of the grains: □, ^{222}Rn from Lipari volcanic glass (Ref. 9); △, ^{222}Rn, and ◇, ^{220}Rn from pitchblende (Ref. 10).

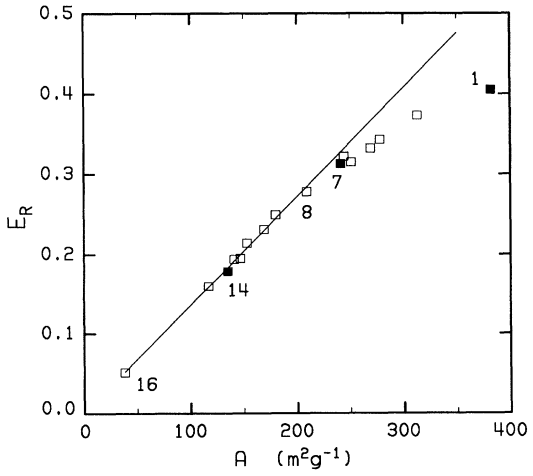

FIG. 4. Emanating power E_R plotted vs the specific surface area A for ^{220}Rn from MgO (Ref. 11).

timation of the fractal dimensions for points number 14, 7, and 1, by fitting the fractal BET model[12] to the reported adsorption data:[11] We obtained $D \approx 2.4$, 2.6, and 2.9, respectively. Also, the grain sizes appear to be decreasing for points 14, 7, and 1, respectively, on the basis of the reported electron micrographs.[11] Using the fractal Eq. (8a) and the values of D above, the theory/experiment ratios of slopes drop to 4.5, 2.7, and 1.5 for points 14, 7 and 1, respectively. The remaining discrepancy factor of 1.5–4.5 is attributed to Rn loss due to implantation in the solid. Thamer, Nielson, and Felthauser[13] studied the effects of water in Rn emanation from rocks [i.e., $E_R(\text{wet})/E_R(\text{dry})$]. They found a range of water effects between 1.4 and 4.1. Because the recoils are believed to stop in water rather than implant, these data support the fractal model with implantation.

The Rn atoms recoiling from the surface have a distribution of kinetic energies from 0 to E_0 keV depending on the position of α decay under the surface. They can implant in the same surface, such as indicated by arrow 2 in Fig. 2, or into a neighbor grain, if the interstitial separation between the grains is smaller than the recoil range in the air. Considering the emanation from the plate and implantation into another plate the net emanating power is given by

$$E_R = \frac{1}{4}\frac{E_t}{E_0}\frac{R_m}{r_0}, \tag{10}$$

where E_t is a threshold energy for implantation. Thus E_R would be reduced by a factor E_0/E_t due to implantation. E_t does not have a fixed value and the sticking probability ranges from $\sim 10^{-5}$ at eV energies to ~ 0.6 at 3 keV and is equal to 1 for energies ≥ 5 keV.[14] Using $E_0 = 103$ keV and $E_t \approx 3$ keV we get a reduction factor of ~ 34, much higher than that observed above (1.5–4.5). There are two ways of explaining this: with the help of indirect recoil or penetrating recoil, shown as arrows 3 and 4 in Fig. 2, respectively. The concept of indirect recoil[15] assumes that part of the Rn can diffuse out from implantation sites through the radiation-damaged zone (damage diffusion). The experimental evidence suggests, however, that this process occurs only for energies ≤ 5 keV.[14] We therefore suggest that it is the penetrating recoils from Fig. 2 (arrow 4) that are responsible. With an increase of D from 2.4 to 2.9, surface roughness increases and the surface acquires a large number of small irregularities. The recoiling Rn atoms can penetrate these irregularities through losing their energy. This process diminishes the implantation and the ratio of theoretical to experimental slopes decreases from 4.5 to 1.5. The concept of penetrating recoil is also consistent with the emanation of ^{220,222}Rn from pitchblende (Fig. 3). From Eq. (9), $E_R(^{220}\text{Rn})/E_R(^{222}\text{Rn})$ is expected to be $[R_m(^{220}\text{Rn})/R_m(^{222}\text{Rn})]^{3-D}$ or 1.03. The experimental ratio is 1.84. We attribute this high ratio to the fact that ^{220}Rn atoms, having higher ranges, penetrate through more surface irregularities for this high $D = 2.83$, and thus more of them emanate.

The author wishes to thank C. O. Kunz, P. P. Parekh, and A. B. Tanner for stimulating discussions and suggestions as well as C. D. Schwenker for programming support.

[1] *Radon and Its Decay Products in Indoor Air,* edited by W. W. Nazaroff and A. V. Nero (Wiley, New York, 1988).

[2] T. M. Semkow, Geochim. Cosmochim. Acta **54**, 425 (1990); T. M. Semkow and P. P. Parekh, Geophys. Res. Lett. **17**, 837 (1990), and references therein.

[3] S. Flügge and K. E. Zimens, Z. Phys. Chem. B **42**, 179 (1939).

[4] T. M. Semkow, P. P. Parekh, C. O. Kunz, and C. D. Schwenker, in Proceedings of the U.S. Environmental Protection Agency International Symposium on Radon and Radon Reduction Technology, Philadelphia, April 1991 (to be published).

[5] B. B. Mandelbrot, *The Fractal Geometry of Nature* (Freeman, New York, 1983).

[6] I. S. Gradshteyn and I. M. Ryzhik, *Table of Integrals, Series and Products* (Academic, San Diego, 1980).

[7] J. Lindhard and M. Scharff, Phys. Rev. **124**, 128 (1961.

[8] P. Pfeifer, Y. J. Wu, M. W. Cole, and J. Krim, Phys. Rev. Lett. **62**, 1997 (1989).

[9] P. M. de C. Barretto, Ph.D. thesis, Rice University, Houston, Texas, 1972 (unpublished).

[10] I. E. Starik and O. S. Melikova, Radiokhimya **1**, 196 (1959).

[11] C. Quet and P. Bussière, J. Chim. Phys. **72**, 823 (1975).

[12] P. Pfeifer, M. Obert, and M. W. Cole, Proc. Roy. Soc. London A **423**, 169 (1989).

[13] B. J. Thamer, K. K. Nielson, and K. Felthauser, U.S. Department of Commerce, National Technical Information Service Report No. PB83-136358, 1981 (unpublished).

[14] E. V. Kornelsen, Can. J. Phys. **42**, 364 (1964); F. Brown and J. A. Davies, Can. J. Phys. **41**, 844 (1963).

[15] K. E. Zimens, Z. Phys. Chem. A **192**, 1 (1943).